Distributed Model-Free Adaptive Predictive Control for Urban Traffic Networks

Li, Dai; De Schutter, Bart

DOI
10.1109/TCST.2021.3059460

Publication date
2022

Document Version
Final published version

Published in
IEEE Transactions on Control Systems Technology

Distributed Model-Free Adaptive Predictive Control for Urban Traffic Networks

Dai Li and Bart De Schutter, *Fellow, IEEE*

***Abstract*— Data-driven control without using mathematical models is a promising research direction for urban traffic control due to the massive amounts of traffic data generated every day. This article proposes a novel distributed model-free adaptive predictive control (D-MFAPC) approach for multiregion urban traffic networks. More specifically, the traffic dynamics of the network regions are first transformed into MFAPC data models, and then, the derived MFAPC data models instead of mathematical traffic models serve as the prediction models in the distributed control design. The formulated control problem is finally solved with an alternating direction method of multipliers (ADMM)-based approach. The simulation results for the traffic network of Linfen, Shanxi, China, show the feasibility and effectiveness of the proposed method.**

***Index Terms*— Data-driven control, distributed model predictive control (DMPC), macroscopic fundamental diagram (MFD), model-free adaptive predictive control (MFAPC), urban traffic network control.**

I. Introduction

TRAFFIC congestion is a severe problem in urban traffic networks due to the rapid growth of vehicle numbers, and how to deal with traffic congestion problems using the existing traffic infrastructure is still a highly relevant topic. Network-wide traffic control is an excellent way to deal with urban traffic congestion.

Network-wide traffic control optimizes the signal settings of all intersections simultaneously aiming to obtain the globally optimal performance of the entire network. Several approaches for network-wide urban traffic control have been proposed, in which many control and optimization theories are utilized. Some commercial traffic control systems, such as MAXBAND [1] and TRANSYT [2], have been implemented in many cities for a long time. For the traffic-responsive urban control (TUC) strategy [3] and its extended versions [4], [5], a linear quadratic regulator is utilized to balance the traffic flows within the network. To better cope with the fluctuations of traffic flows and to avoid a myopic strategy in the control process, model predictive control (MPC)-based urban traffic control methods were designed utilizing different mathematical traffic models, such as the S model [6], [7] and the store-and-forward model [8], [9]. Robust control was applied in urban traffic control to cope with uncertainty of traffic parameters in [10] and [11].

Although the global optimum can be obtained through network-wide control approaches, computation speed and reliability are always major problems. In this case, a hierarchical or distributed control structure is more practical. A real-time urban traffic control system with a three-level hierarchical structure was proposed in [12]. In [13], a multiagent control approach for urban traffic networks was designed, and convergence of the algorithm was proved. Distributed MPC (DMPC) was adopted to deal with the interactions and negotiations among the network regions in [14]–[16]. However, for these distributed traffic control strategies, detailed mathematical models of the traffic network are needed, which makes them hard to use and to implement in practice. Modeling the traffic dynamics for a given network region is quite difficult, and sometimes, it is impossible. Moreover, even if a mathematical model is available, it is in general not an accurate one, and lots of uncertainties exist, which will definitely deteriorate the control performance when we use the model in practice.

In order to address the traffic congestion problem while making use of the valuable traffic data generated in real-world traffic systems instead of a model-based control method, a novel model-free adaptive predictive control (MFAPC) scheme can be utilized in urban traffic control. MFAPC is extended from model-free adaptive control (MFAC), which is a pure data-driven control approach. MFAC was originally proposed in [17], and it has been developed to cope with control problems for a class of unknown, nonlinear, nonaffine systems based on different dynamic linearization data models using a novel concept of pseudopartial derivative, which can be estimated directly from input–output data [18]. The applications of MFAC include wireless communication systems [19], implantable heart pumps [20], nonlinear distillation columns [21], perimeter control for one-region [22] and multiregion [23], [24] urban traffic networks, and so on. MFAPC is a predictive control scheme derived by embedding the MFAC scheme in a rolling horizon framework [18]. For more detailed discussions on MFAC, we refer the interested readers to [25] and [26].

In [23] and [24], MFAC-based perimeter control strategies for multiregion urban traffic networks were proposed aiming to

Manuscript received December 19, 2020; accepted February 8, 2021. Date of publication March 2, 2021; date of current version December 15, 2021. Manuscript received in final form February 11, 2021. This work was supported by the National Natural Science Foundation of China under Grant 61433002 and Grant 61833001. Recommended by Associate Editor M. Dotoli. *(Corresponding author: Dai Li.)*

Dai Li is with the Advanced Control Systems Laboratory, School of Electronic and Information Engineering, Beijing Jiaotong University, Beijing 100044, China (e-mail: 15111014@bjtu.edu.cn).

Bart De Schutter is with the Delft Center for Systems and Control, Delft University of Technology, 2628 CD Delft, The Netherlands (e-mail: b.deschutter@tudelft.nl).

Color versions of one or more figures in this article are available at https://doi.org/10.1109/TCST.2021.3059460.

Digital Object Identifier 10.1109/TCST.2021.3059460

make the number of vehicles in each region track a set point by metering the traffic inflows and outflows among the regions. However, there are two deficiencies in these two methods. First, only the macroscopic interactions among the regions are considered, while the traffic dynamics in the intersection and link level, and the detailed signal settings of the traffic lights are not considered. Furthermore, there is no negotiation mechanism for the interactions among the regions, which leads to a nonglobal and noncooperative perspective in the control process.

In order to deal with the interactions among the network regions, the DMPC approach, which is a general control methodology that can tackle the distributed control problem of large-scale systems, can be utilized. The basic concept, research results, and research directions of DMPC are discussed in, e.g., [27] and [28]. To solve DMPC problems, the augmented Lagrangian relaxation (ALR) [29] and the alternating direction method of multipliers (ADMM)-based [30] approaches are widely used. DMPC has been applied in power systems [31], wind farms [32], synchromodal freight transport [33], and urban traffic control [14]–[16]. However, note that all these approaches require a mathematical model of the system as prediction model.

In this article, a distributed model-free adaptive predictive control (D-MFAPC) strategy for multiregion urban traffic networks is proposed. First, we derive the MFAPC data models of the network regions by analyzing the traffic dynamics of the network. Then, we design the D-MFAPC algorithm based on the derived MFAPC data models in a distributed control structure. To deal with traffic flow interactions and negotiations among the regions, the formulated D-MFAPC problem is solved with the ADMM-based DMPC approach.

The contributions of this article are summarized as follows.

1) Under the assumptions of congested traffic condition and equalized cycle length among the intersections, the MFAPC data models [18] of the multiregion urban traffic networks are derived. By using the MFAPC data models, the traffic controller can be designed only using the measured data of the traffic networks without the need of precise mathematical models.
2) The D-MFAPC strategy for multiregion urban traffic networks is designed based on the derived MFAPC data models. Different from model-based distributed urban traffic control [14]–[16], the derived MFAPC data models instead of traffic mathematics models are utilized in the control process, which can avoid model mismatch and decrease the computational effort.
3) Compared with the existing MFAC-based traffic control methods for multiregion networks [23], [24], besides the macroscopic interactions among the regions, the detailed traffic signal settings in the traffic network are also considered. Furthermore, a negotiation mechanism using the ADMM-based approach [30], [33] is designed to enhance the globality and cooperativeness of the distributed controllers.

The rest of this article is organized as follows. In Section II, notations on multiregion urban traffic networks are introduced, and the traffic dynamics of the regions are analyzed. Then, MFAPC data models of the traffic networks and the D-MFAPC strategy are presented in Section III. Next, a case study is carried out to verify the proposed control method in Section IV. Finally, Section V concludes this article.

To facilitate the description of the proposed control approach, the following notations are presented. First, $X \cap Y$ and $X \cup Y$ stand for the intersection and the union of sets X and Y, respectively, $|x|$ is the absolute value of a scalar x, and $\|\mathbf{x}\|_2$ indicates the 2-norm of a vector $\mathbf{x}$. Then, we denote k as the time index of the traffic system and define $\bar{\mathbf{x}}(k) = [\mathbf{x}^{\mathrm{T}}(k), \mathbf{x}^{\mathrm{T}}(k-1), \ldots, \mathbf{x}^{\mathrm{T}}(1)]^{\mathrm{T}}$ for a vector $\mathbf{x}(k)$ at time step k. Furthermore, the variables that will be used in the remainder of this article are summarized in Table I.

II. Dynamics of Urban Traffic Networks

A. Multiregion Urban Traffic Networks

Assume that a traffic network is decomposed into several regions, for which many traffic network decomposition methods can be utilized (see [34]–[36]). An illustrative example of a network composed of two regions is shown in Fig. 1, where $V = \{V_1, V_2, V_3, V_4\}$ is the set of vehicle inflow points of the network from which the traffic demands are generated.

Next, some notations on intersections and links are introduced. We denote I as the set of intersections in the network. Two intersections are called neighbors if they are connected through a link, e.g., for Fig. 1(b), $I_i^{\mathrm{N}} = \{j_1, j_2, j_3, j_4\}$, where I_i^{N} is the set of neighboring intersections of intersection i. The pair (j, i) represents the link on which vehicles travel from intersection j to intersection i. Moreover, I_r is the set of intersections in region r, $r = 1, 2$, I_r^{B} is the set of intersections in region r at the boundary of the network, and $I_{r,\bar{r}}^{\mathrm{B}}$ is the set of intersections in region r at the boundary with another region $\bar{r}$. In Fig. 1(a), I_1, I_2, I_1^{B}, I_2^{B}, $I_{1,2}^{\mathrm{B}}$, and $I_{2,1}^{\mathrm{B}}$ are given by

$$I_1 = \{1, 2, 3, 4, 5, 6\}, \quad I_1^{\mathrm{B}} = \{1, 4\}, I_{1,2}^{\mathrm{B}} = \{3, 6\}$$
$$I_2 = \{7, 8, 9, 10\}, \quad I_2^{\mathrm{B}} = \{8, 10\}, I_{2,1}^{\mathrm{B}} = \{7, 9\}.$$

A signal phase of an intersection is a period of time during which a specific set of traffic flows are allowed to cross the intersection. We define $\mathbf{g}_i(k) \in \mathbf{R}^{p_i}$ as the vector of phase green times of intersection i at time step k, which can be described as

$$\mathbf{g}_i(k) = \left[g_{i,1}(k), \ldots, g_{i,p_i}(k)\right]^{\mathrm{T}} \tag{1}$$

where p_i is the number of signal phases of intersection i.

Assume that all intersections in the network have the same cycle length T, i.e.,

$$g_{i,1}(k) + \cdots + g_{i,p_i}(k) = T - L_i \tag{2}$$

where L_i is the total lost time of intersection i within a signal cycle which is imposed to avoid interference among incompatible traffic flows of consecutive signal phases. This assumption is introduced to facilitate the analysis of the traffic dynamics in Section II-B.

Remark 1: In this article, we take the two-region urban traffic network as an illustrative example just to simplify the description of the proposed D-MFAPC approach. However,

TABLE I
LIST OF VARIABLES

Variable	Definition
I	set of intersections in the network
I_i^{N}	set of neighboring intersections of intersection i
I_r	set of intersections in region r
I_r^{B}	set of intersections in region r that are at the boundary of the network
$I_{r,\bar{r}}^{\mathrm{B}}$	set of intersections in region r that are at the boundary with another region $\bar{r}$
V	set of vehicle inflow points of the traffic network
M	prediction and control horizon of the traffic controller
T	sampling interval and common cycle length of all intersections in the network
$e_{(j,i)}(k)$	number of vehicles entering link (j,i) at time step k
$e_r(k)$	number of vehicles entering region r at time step k
$e(k)$	number of vehicles entering the traffic network at time step k
$l_{(j,i)}(k)$	number of vehicles leaving link (j,i) at time step k
$l_{(j,i,m)}(k)$	number of vehicles leaving link (j,i) towards link (i,m) at time step k
$l_r(k)$	number of vehicles leaving region r at time step k
$l(k)$	number of vehicles leaving the traffic network at time step k
$n_{(j,i)}(k)$	number of vehicles on link (j,i) at time step k
$n_r(k)$	number of vehicles in region r at time step k
$\mathbf{\Theta}_r(k)$	$=[n_r(k),\cdots,n_r(k+M-1)]^{\mathrm{T}}$
n_r^{set}	set point of number of vehicles in region r
$\mathbf{N}_r(k)$	vector of the number of vehicles of the links in region r at time step k
$\mathbf{N}_{r,\bar{r}}(k)$	vector of the number of vehicles of the links on which vehicles travel from region r to region $\bar{r}$ at time step k
$\mathbf{g}_i(k)$	vector of phase green times of intersection i at time step k
$\mathbf{G}_r(k)$	vector of green splits of all intersections in region r at time step k
$\mathbf{G}_{r,\bar{r}}^{\mathrm{B}}(k)$	vector of green splits of intersections in region r that are at the boundary with region $\bar{r}$ at time step k
$z_{\bar{r},r}(k)$	interaction input of region r caused by region $\bar{r}$ at time step k
$y_{r,\bar{r}}(k)$	interaction output of region r on region $\bar{r}$ at time step k
$\mathbf{Z}_{\bar{r},r}(k)$	$=[z_{\bar{r},r}(k),\cdots,z_{\bar{r},r}(k+M-1)]^{\mathrm{T}}$
$\mathbf{Y}_{r,\bar{r}}(k)$	$=[y_{r,\bar{r}}(k),\cdots,y_{r,\bar{r}}(k+M-1)]^{\mathrm{T}}$
$\mathbf{u}_r(k)$	$=\left[\mathbf{G}_r^{\mathrm{T}}(k),\mathbf{N}_r^{\mathrm{T}}(k),\mathbf{N}_{r,\bar{r}}^{\mathrm{T}}(k),z_{\bar{r},r}(k)\right]^{\mathrm{T}}$
$\mathbf{u}_{r,\bar{r}}(k)$	$=\left[\left(\mathbf{G}_{r,\bar{r}}^{\mathrm{B}}(k)\right)^{\mathrm{T}},\mathbf{N}_{r,\bar{r}}^{\mathrm{T}}(k)\right]^{\mathrm{T}}$
$\mathbf{U}_r(k)$	$=\left[\Delta\mathbf{u}_{r,\bar{r}}^{\mathrm{T}}(k),\cdots,\Delta\mathbf{u}_{r,\bar{r}}^{\mathrm{T}}(k+M-1)\right]^{\mathrm{T}}$
$\mathbf{U}_{r,\bar{r}}(k)$	$=\left[\Delta\mathbf{u}_r^{\mathrm{T}}(k),\cdots,\Delta\mathbf{u}_r^{\mathrm{T}}(k+M-1)\right]^{\mathrm{T}}$
$\boldsymbol{\phi}_r(k)$	pseudo-gradient of the MFAC data model of $n_r(k)$
$\boldsymbol{\varphi}_{r,\bar{r}}(k)$	pseudo-gradient of the MFAC data model of $y_{r,\bar{r}}(k)$
$\mathbf{A}_r(k)$	matrix composed of $\phi_r(k+i)$, $i=0,\cdots,M-1$
$\mathbf{A}_{r,\bar{r}}(k)$	matrix composed of $\varphi_{r,\bar{r}}(k+i)$, $i=0,\cdots,M-1$
$\lambda_{\mathrm{in},\bar{r},r}^s(k)$	Lagrangian multiplier of interaction input of region r caused by region $\bar{r}$ at time step k, iteration s
$\lambda_{\mathrm{out},r,\bar{r}}^s(k)$	Lagrangian multiplier of interaction output of region r on region $\bar{r}$ at time step k, iteration s

it should be emphasized that the D-MFAPC approach can be easily extended to traffic networks composed of more than two regions.

B. Analysis of Traffic Dynamics of Multiregion Networks

Let the sampling interval of the traffic system be equal to the common cycle length T. Then, the dynamics of the number of vehicles in the network, in region r, and on link (j,i) can be described as

$$n(k+1)=n(k)+e(k)-l(k) \tag{3}$$

$$n_r(k+1)=n_r(k)+e_r(k)-l_r(k) \tag{4}$$

$$n_{(j,i)}(k+1)=n_{(j,i)}(k)+e_{(j,i)}(k)-l_{(j,i)}(k) \tag{5}$$

where $e(k)$ and $l(k)$ are the number of vehicles entering and leaving the network, respectively, at time step k; $e_r(k)$ and $l_r(k)$ are the number of vehicles entering and leaving region r, respectively, at time step k; and $e_{(j,i)}(k)$ and $l_{(j,i)}(k)$ are the number of vehicles entering and leaving link (j,i), respectively, at time step k.

In this article, we adopt the S model [7], [37], which gives a good balance between accuracy and computation speed, to describe the dynamics of $e_{(j,i)}(k)$ and $l_{(j,i)}(k)$. However, note that other mathematical traffic models, such as the store-and-forward model [3], [38] and the BLX model [39], [40], can also be utilized instead. In the S model, $e_{(j,i)}(k)$ is expressed as the sum of number of vehicles leaving from upstream links of link (j,i), while $l_{(j,i)}(k)$ depends on the signal settings of intersection i, the number of queuing vehicles, and vehicles arriving at the tail of the queue on link (j,i), and the remaining capacity of the downstream links of link (j,i) at time step k. Interested readers are referred to [7] and [37] for a detailed description of the S model.

Assumption 1: We assume that the traffic capacity outside the network is large enough so that there is no backpropagation of congestion from outside the network to inside the network, and the external traffic inflow rates generated from the vehicle inflow points are known or accurately predictable for all time steps. Furthermore, we assume that the network is congested, and the vehicles cannot cross two consecutive intersections within one signal cycle.

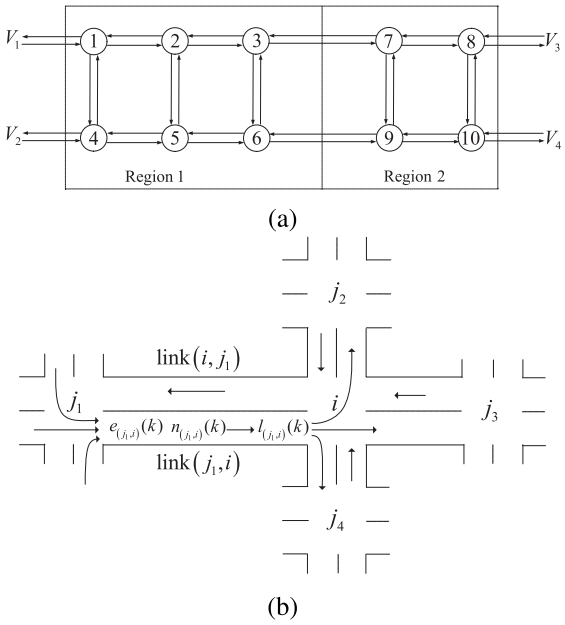

Fig. 1. Illustrative example of a two-region urban traffic network. (a) Decomposition of the traffic network. (b) Diagram of intersections and links.

Remark 2: The above assumptions of unlimited capacity outside the network and known traffic inflow are made to help us rule out traffic interference from outside the network and to focus on the traffic dynamics inside. While under the assumption that the network is congested, we do not need to consider the queuing vehicles and vehicles arriving at the tail of the queue of link (j,i) anymore. This can reduce the number of traffic variables and simplify the analysis of the S model and the derived MFAPC data model that will be elaborated next; this assumption is also acceptable in practical applications, as real-time traffic signal optimization is only necessary when the traffic network is congested.

Regarding Assumption 1, $e_{(j,i)}(k)$ and $l_{(j,i)}(k)$ in (5) are expressed as follows according to the S model:

$$\begin{cases} e_{(j,i)}(k) = \displaystyle\sum_{m\in I_{\mathrm{N},j}, m\neq i} \min\left(\frac{\mu_{(m,j,i)} g_{i,p(m,j,i)}(k)}{T}, \right. \\ \qquad\qquad \left. \dfrac{\beta_{(m,j,i)}\left(C_{(j,i)} - n_{(j,i)}(k)\right)}{T}\right) \\ \qquad\qquad\qquad\qquad \text{for } j \in I \\ e_{(j,i)}(k) = \min\left(v_j(k), \dfrac{C_{(j,i)} - n_{(j,i)}(k)}{T}\right) \quad \text{for } j \in V \end{cases} \tag{6}$$

$$\begin{cases} l_{(j,i)}(k) = \displaystyle\sum_{m\in I_{\mathrm{N},i}, j\neq m} l_{(j,i,m)}(k) \\ l_{(j,i,m)}(k) = \min\left(\dfrac{\mu_{(j,i,m)} g_{i,p_{(j,i,m)}}(k)}{T}, \right. \\ \qquad\qquad \left. \dfrac{\beta_{(j,i,m)}\left(C_{(i,m)} - n_{(i,m)}(k)\right)}{T}\right) \quad \text{for } m \in I \\ l_{(j,i,m)}(k) = \dfrac{\mu_{(j,i)} g_{i,p_{(j,i,m)}}(k)}{T} \qquad\qquad \text{for } m \in V \end{cases} \tag{7}$$

where $l_{(j,i,m)}(k)$ is the number of vehicles leaving link (j,i) toward link (i,m), $\beta_{(j,i,m)}$ is the ratio of vehicles going from link (j,i) toward link (i,m), $\mu_{(j,i,m)}$ is the saturation flow rate leaving link (j,i) toward link (i,m), $p_{(j,i,m)}$ is the index number of signal phase of intersection i for traffic flow from link (j,i) toward link (i,m), $C_{(j,i)}$ is the capacity of link (j,i) measured in number of vehicles, and $v_j(k)$ is the number of vehicles generated by vehicle inflow point $j \in V$ at time step k which is known or accurately predictable as mentioned in Assumption 1.

The expressions of $e_{(j,i)}(k)$ and $l_{(j,i,m)}(k)$ can be written compactly as

$$\begin{cases} e_{(j,i)}(k) = f^{\mathrm{I}}_{\mathrm{E},(j,i)}\left(\mathbf{g}_j(k), n_{(i,j)}(k)\right), & \text{for } j \in I \\ e_{(j,i)}(k) = f^{\mathrm{B}}_{\mathrm{E},(j,i)}\left(n_{(i,j)}(k)\right), & \text{for } j \in V \end{cases} \tag{8}$$

$$\begin{cases} l_{(j,i,m)}(k) = f^{\mathrm{I}}_{\mathrm{L},(j,i,m)}\left(\mathbf{g}_i(k), n_{(i,m)}(k)\right), & \text{for } m \in I \\ l_{(j,i,m)}(k) = f^{\mathrm{B}}_{\mathrm{L},(j,i,m)}\left(\mathbf{g}_i(k)\right), & \text{for } m \in V \end{cases} \tag{9}$$

for appropriately defined functions $f^{\mathrm{I}}_{\mathrm{E},(j,i)}(\cdot)$, $f^{\mathrm{B}}_{\mathrm{E},(j,i)}(\cdot)$, $f^{\mathrm{I}}_{\mathrm{L},(j,i,m)}(\cdot)$, and $f^{\mathrm{B}}_{\mathrm{L},(j,i,m)}(\cdot)$.

Then $e_r(k)$ can be expressed as follows based on (4)–(9):

$$\begin{aligned} e_r(k) &= \sum_{j\in V, i\in I^{\mathrm{B}}_r} e_{(j,i)}(k) + \sum_{j\in I^{\mathrm{B}}_{\bar{r},r}, i\in I^{\mathrm{B}}_{r,\bar{r}}} e_{(j,i)}(k) \\ &= \sum_{j\in V, i\in I^{\mathrm{B}}_r} f^{\mathrm{B}}_{\mathrm{E},(j,i)}\left(n_{(j,i)}(k)\right) + z_{\bar{r},r}(k) \\ &= \sum_{j\in V, i\in I^{\mathrm{B}}_r} f^{\mathrm{B}}_{\mathrm{E},(j,i)}\left(n_{(j,i)}(k-1), l_{(j,i)}(k-1)\right. \\ &\quad \left. e_{(j,i)}(k-1)\right) + z_{\bar{r},r}(k) \\ &= \sum_{\substack{j\in V \\ i\in I^{\mathrm{B}}_r, m\in I^{\mathrm{N}}_i}} f^{\mathrm{B}}_{\mathrm{E},(j,i)}\left(n_{(j,i)}(k-1), \mathbf{g}_i(k-1)\right. \\ &\quad \left. n_{(i,m)}(k-1)\right) + z_{\bar{r},r}(k) \end{aligned} \tag{10}$$

for $r = 1, 2$ with $\bar{r} = 3 - r$, and where $z_{\bar{r},r}(k)$ is the interaction input of region r caused by another region $\bar{r}$. The first term of (10) is the number of vehicles generated from the vehicle inflow points, and the second term is the number of vehicles leaving from region $\bar{r}$ for region r. Then, $n_{(i,m)}(k)$ in (10) can be further expressed as follows according to (4)–(9):

$$\begin{aligned} & n_{(i,m)}(k) \\ &= n_{(i,m)}(k-1) - l_{(i,m)}(k-1) + e_{(i,m)}(k-1) \\ &= n_{(i,m)}(k-1) - f^{\mathrm{I}}_{\mathrm{L},(i,m,o)}\left(\mathbf{g}_m(k-1), n_{(m,o)}(k-1)\right) \\ &\quad + f^{\mathrm{I}}_{\mathrm{E},(i,m)}\left(\mathbf{g}_i(k-1), n_{(i,m)}(k-1)\right) \\ &\quad \text{for } o \in I^{\mathrm{N}}_m \cap I_r \\ &= f_{(i,m)}\left(n_{(i,m)}(k-1), \mathbf{g}_i(k-1), n_{(m,o)}(k-1), \mathbf{g}_m(k-1)\right) \\ &= f_{(i,m)}\left(n_{(i,m)}(k-1), \mathbf{g}_i(k-1), \mathbf{g}_m(k-1), n_{(m,o)}(k-2)\right. \\ &= n_{(o,w)}(k-2), \mathbf{g}_m(k-2), \mathbf{g}_o(k-2)\big) \\ &\quad \text{for } w \in I^{\mathrm{N}}_o \cap I_r \\ &= f_{(i,m)}\left(\tilde{\mathbf{G}}_r(k), \tilde{\mathbf{N}}_r(k)\right) \end{aligned} \tag{11}$$

where $\mathbf{G}_r(k) = [\mathbf{g}_i(k)]_{i\in I_r}$ and $\mathbf{N}_r(k) = [n_{(j,i)}(k)]_{i\in I_r, j\in I^{\mathrm{N}}_i}$ are the vector of green times of all intersections in region r, and the vector of number of vehicles on all links in region r respectively. Based on (10) and (11), we can get

$$e_r(k) = f_{\mathrm{enter}}\left(\tilde{\mathbf{G}}_r(k), \tilde{\mathbf{N}}_r(k), z_{r,\bar{r}}(k)\right). \tag{12}$$

Similar to $e_r(k)$, $l_r(k)$ can be divided into the vehicles leaving the network and the vehicles leaving region r for region $\bar{r}$

$$\begin{aligned} l_r(k) &= \sum_{m\in I^{\mathrm{N}}_j} \sum_{j\in I^{\mathrm{B}}_r, i\in V} l_{(m,j,i)}(k) \\ &\quad + \sum_{m\in I^{\mathrm{N}}_j} \sum_{j\in I^{\mathrm{B}}_{r,\bar{r}}, i\in I^{\mathrm{B}}_{\bar{r},r}} l_{(m,j,i)}(k) \\ &= \sum_{j\in I^{\mathrm{B}}_{r,\bar{r}}, i\in I^{\mathrm{B}}_{\bar{r},r}} f^{\mathrm{I}}_{\mathrm{L},(m,j,i)}\left(n_{(j,i)}(k), \mathbf{g}_j(k)\right) \\ &\quad + \sum_{j\in I^{\mathrm{B}}_r} f^{\mathrm{B}}_{\mathrm{L},(m,j,i)}\left(\mathbf{g}_j(k)\right) \\ &= f_{\mathrm{leave}}\left(\mathbf{G}^{\mathrm{B}}_r(k), \mathbf{G}^{\mathrm{B}}_{r,\bar{r}}(k), \mathbf{N}_{r,\bar{r}}(k)\right) \end{aligned} \tag{13}$$

where $\mathbf{G}^{\mathrm{B}}_r(k) = [\mathbf{g}_i(k)]_{i\in I^{\mathrm{B}}_r}$ is the vector of phase green times of intersections in region r at the boundary of the

network, $\mathbf{G}^{\mathrm{B}}_{r,\bar{r}}(k) = [\mathbf{g}_i(k)]_{i\in I^{\mathrm{B}}_{r,\bar{r}}}$ is the vector of green times of intersections in region r at the boundary with region $\bar{r}$, and $\mathbf{N}_{r,\bar{r}}(k) = [n_{(j,i)}(k)]_{j\in I_r, i\in I_{\bar{r}}}$ is the vector of number of vehicles on links through which vehicles can travel from region r to region $\bar{r}$.

Similarly, $e(k)$ and $l(k)$ can be expressed, respectively, as

$$\begin{aligned} e(k) &= \sum_{j\in V, i\in I^{\mathrm{B}}_r} e_{(j,i)}(k) \\ &= \bar{f}_{\mathrm{enter}}\big(\tilde{\mathbf{G}}_r(k), \tilde{\mathbf{N}}_r(k)\big) \end{aligned} \tag{14}$$

$$\begin{aligned} l(k) &= \sum_{m\in I^{\mathrm{N}}_j} \sum_{j\in I^{\mathrm{B}}_r, i\in V} l_{(m,j,i)}(k) \\ &= \bar{f}_{\mathrm{leave}}\big(\mathbf{G}^{\mathrm{B}}_r(k)\big). \end{aligned} \tag{15}$$

Based on (9), the interaction output of region r on another region $\bar{r}$ (number of vehicles leaving region r for region $\bar{r}$) at time step k is calculated as

$$\begin{aligned} y_{r,\bar{r}}(k) &= \sum_{m\in I^{\mathrm{N}}_j} \sum_{j\in I^{\mathrm{B}}_{r,\bar{r}}, i\in I^{\mathrm{B}}_{\bar{r},r}} l_{(m,j,i)}(k) \\ &= \sum_{j\in I^{\mathrm{B}}_{r,\bar{r}}, i\in I^{\mathrm{B}}_{\bar{r},r}} f^{\mathrm{I}}_{\mathrm{L},(m,j,i)}\big(n_{(j,i)}(k), \mathbf{g}_j(k)\big) \\ &= f_y\big(\mathbf{G}^{\mathrm{B}}_{r,\bar{r}}(k), \mathbf{N}_{r,\bar{r}}(k)\big). \end{aligned} \tag{16}$$

It is important to note that the traffic dynamics for $n_r(k)$ and $y_{r,\bar{r}}(k)$ presented in (4), (10)–(13), and (16) are just utilized to present the basic traffic dynamics and that they are not involved in the controller design. This is because they are highly nonlinear, and an online optimization-based traffic controller designed based on these dynamics would be very complex and time-consuming. Moreover, there are still lots of unmodeled traffic dynamics and uncertainties not reflected in the model. In this case, we can represent the traffic dynamics of $n_r(k)$ and $y_{r,\bar{r}}(k)$ as MFAPC data models and resort to the MFPAC scheme to design the traffic controller as will be explained next.

III. D-MFAPC Strategy for Urban Traffic Networks

A. Control Problem Formulation

The objective of the D-MFAPC strategy is to regulate the number of vehicles in the network $n_r(k)$ tracking the set point n^{set}_r by optimizing $\mathbf{G}_r(k)$, the interaction input $z_{\bar{r},r}(k)$, and the interaction output $y_{r,\bar{r}}(k)$ of each region r; thus, the traffic flow efficiency in the network can be improved.

To deal with the problems of model mismatch and complex computation which always exist in model-based control methods, the MFAPC scheme is adopted. Specifically, the dynamics of $n_r(k)$ and $y_{r,\bar{r}}(k)$ described in (4), (10)–(13), and (16) can be represented by the equivalent dynamic linearized MFAPC data models with the help of the pseudogradients in a rolling horizon framework. The pseudogradients in the linearized dynamic data models are updated by the real-time measured data of the traffic system at each time step k without using any information of the mathematical model. Then, the derived MFAPC data models can be utilized to design the D-MFAPC algorithm.

There are three features of the proposed control method. First, all the nonlinear properties and unmodeled dynamics of original traffic model are fused into the pseudogradients, and thus, no mathematical traffic model is required in the controller design. Second, the MFAPC data model is an equivalent dynamic linearization data model instead of a static approximation model, and no high-order term of the original model is lost. Finally, the MFAPC data model is linear with a very simple structure, which can dramatically decrease the computational burden when we use it in the control process.

B. MFAPC Data Models of the Regions

Considering the two-region urban traffic network in Fig. 1(a), the dynamics of the number of vehicles in region $r, r = 1, 2$ can be represented by a more general form for the MFAPC application based on (4), (12), and (13)

$$n_r(k+1) = f_n(n_r(k),\ldots,n_r(k-\gamma_n), \mathbf{u}_r(k),\ldots,\mathbf{u}_r(k-\gamma_u)) \tag{17}$$

where $\mathbf{u}_r(k) = [\mathbf{G}^{\mathrm{T}}_r(k), \mathbf{N}^{\mathrm{T}}_r(k), \mathbf{N}^{\mathrm{T}}_{r,\bar{r}}(k), z_{\bar{r},r}(k)]^{\mathrm{T}}$, $\bar{r} = 3 - r$, and γ_n and γ_u are the memory lengths of the traffic system for the number of vehicles and the system inputs, respectively.

There are three forms of the MFAC data models: compact form, partial form, and full form dynamic linearized data model [18], [26]. The main difference between these three forms consists in how many past input and output increments are used to model the next output increment.

Without loss of generality and for simplicity, the compact form dynamic linearized (CFDL) data model will be used in this article. Before the CFDL method is elaborated, some assumptions [18], [25], [26] are made on system (17).

Assumption 2: The partial derivatives of $f_n(\cdot)$ in (17) with respect to every entry of the variable $\mathbf{u}_r(k)$ are continuous.

Assumption 3: The above system satisfies the generalized Lipschitz condition.

There exists a positive constant c_r such that

$$|n_r(k_1+1) - n_r(k_2+1)| \le c_r \|\mathbf{u}_r(k_1) - \mathbf{u}_r(k_2)\|_2$$

for $\mathbf{u}_r(k_1) \neq \mathbf{u}_r(k_2)$ for any $k_1, k_2 > 0$ with $k_1 \neq k_2$.

Remark 3: As regards Assumption 2, it should be noted that the partial derivatives of $f_n(\cdot)$ with respect to the entries of $\mathbf{G}_r(k)$ are not always continuous at some specific points because $e_{(j,i)}(k)$ and $l_{(j,i)}(k)$ are min functions of $\mathbf{g}_i(k)$ [see (6) and (7)]; however, we can smooth these min functions utilizing some smoothening methods to make the partial derivatives continuous [41]. Moreover, Assumption 3 is a physical constraint of the inherent nature of urban traffic systems, i.e., finite changes of signal settings and interacted input flow would not lead to infinite change in the number of vehicles in a region.

Then system (17) can be transformed into the following MISO CFDL-MFAC data model [18], [25], [26]:

$$\begin{aligned} n_r(k+1) &= n_r(k) + \boldsymbol{\phi}^{\mathrm{T}}_r(k)\Delta\mathbf{u}_r(k) \\ \boldsymbol{\phi}_r(k) &= \big[\phi_1(k),\ldots,\phi_{q_r}(k),\phi_{q_r+1}(k),\ldots,\phi_{q_r+h_r+1}(k)\big]^{\mathrm{T}} \end{aligned} \tag{18}$$

where $\boldsymbol{\phi}_r(k) \in {}^{q_r+h_r+1}$ is the pseudogradient of the system, q_r is the total number of signal phases in region r, h_r is

the sum of the number of elements in $\mathbf{N}_r(k)$ and $\mathbf{N}_{r,\bar{r}}(k)$, and $\Delta\mathbf{u}_r(k)=\mathbf{u}_r(k)-\mathbf{u}_r(k-1)$. Then, by embedding the derived MFAC data model in an M-step ahead rolling horizon framework, the MFAC data model of the traffic system (18) can be further transformed into the following MFAPC data model [18] for the traffic system:

$$\Theta_r(k+1)=\mathbf{E}n_r(k)+\mathbf{A}_r(k)\Delta\mathbf{U}_r(k) \tag{19}$$

where

$$\begin{aligned}\Theta_r(k+1)&=[n_r(k+1),\ldots,n_r(k+M)]^{\mathrm{T}}\\ \Delta\mathbf{U}_r(k)&=\left[\Delta\mathbf{u}_r^{\mathrm{T}}(k),\ldots,\Delta\mathbf{u}_r^{\mathrm{T}}(k+M-1)\right]^{\mathrm{T}}\\ \mathbf{E}&=\left[\underbrace{1,1,\ldots,1}_{M}\right]^{\mathrm{T}}\\ \mathbf{A}_r(k)&=\begin{bmatrix}\boldsymbol{\phi}_r^{\mathrm{T}}(k) & \mathbf{0}^{\mathrm{T}} & \cdots & \mathbf{0}^{\mathrm{T}}\\ \boldsymbol{\phi}_r^{\mathrm{T}}(k) & \boldsymbol{\phi}_r^{\mathrm{T}}(k+1) & \cdots & \mathbf{0}^{\mathrm{T}}\\ \vdots & \vdots & \ddots & \vdots\\ \underbrace{\boldsymbol{\phi}_r^{\mathrm{T}}(k) & \boldsymbol{\phi}_r^{\mathrm{T}}(k+1) & \cdots & \boldsymbol{\phi}_r^{\mathrm{T}}(k+M-1)}_{M\times[(q_r+h_r+1)M]}\end{bmatrix}.\end{aligned}$$

It should be noted that $\mathbf{A}_r(k)$ contains the unknown system pseudogradients, as seen in (19), and therefore, estimation and forecasting algorithms are needed. Considering the following cost function of $\boldsymbol{\phi}_r(k)$ [18], [25], [26]:

$$\begin{aligned}J\left(\boldsymbol{\phi}_r(k)\right)=&\left|n_r(k)-n_r(k-1)-\boldsymbol{\phi}_r^{\mathrm{T}}(k)\Delta\mathbf{u}_r(k-1)\right|^2\\&+\mu_r\left\|\boldsymbol{\phi}_r(k)-\hat{\boldsymbol{\phi}}_r(k-1)\right\|_2^2\end{aligned} \tag{20}$$

where $\mu_r>0$ is used to restrict the change of pseudogradient, and $\hat{\boldsymbol{\phi}}_r(k)$ is the estimation of $\boldsymbol{\phi}_r(k)$. The first term of (20) is the difference between the true measured number of vehicles in region r and the CFDL data model output, whereas the second term penalizes large variations of the pseudogradient, which intends to enhance the robustness of the estimation algorithm to disturbances and outliers. The pseudogradient $\boldsymbol{\phi}_r(k)$ can be estimated by minimizing (20) with respect to $\boldsymbol{\phi}_r(k)$

$$\begin{aligned}\hat{\boldsymbol{\phi}}_r(k)=&\hat{\boldsymbol{\phi}}_r(k-1)+\frac{\eta_r\Delta\mathbf{u}_r(k-1)}{\mu_r+\|\Delta\mathbf{u}_r(k-1)\|_2^2}\\&\left(n_r(k)-n_r(k-1)-\hat{\boldsymbol{\phi}}_r^{\mathrm{T}}(k-1)\Delta\mathbf{u}_r(k-1)\right)\end{aligned} \tag{21}$$

where $\eta_r\in(0,1]$. However, the estimates of $\boldsymbol{\phi}_r(k+1)$, …, $\boldsymbol{\phi}_r(k+M-1)$ cannot be directly obtained utilizing the input and output data at time step k. Therefore, we adopt a multilayer hierarchical forecasting method [18], [42] to forecast these pseudogradients, which is given as

$$\begin{aligned}\hat{\boldsymbol{\phi}}_r(k+i)=&\theta_1(k)\hat{\boldsymbol{\phi}}_r(k+i-1)+\theta_2(k)\hat{\boldsymbol{\phi}}_r(k+i-2)\\&+\cdots+\theta_m(k)\hat{\boldsymbol{\phi}}_r(k+i-m)\\&i=1,\ldots,M-1\end{aligned} \tag{22}$$

where m is a properly selected order whose value is normally set as $2-7$ [18], [42].

Define $\boldsymbol{\theta}(k)=[\theta_1(k),\ldots,\theta_m(k)]^{\mathrm{T}}$. This vector can be determined using the following equation [18], [42]:

$$\boldsymbol{\theta}(k)=\boldsymbol{\theta}(k-1)+\frac{\hat{\Phi}^{\mathrm{T}}(k-1)}{\delta+\left\|\hat{\Phi}(k-1)\right\|_2}\left[\hat{\boldsymbol{\phi}}_r(k)-\hat{\Phi}(k-1)\boldsymbol{\theta}(k-1)\right] \tag{23}$$

where $\hat{\Phi}(k-1)=[\hat{\boldsymbol{\phi}}_r(k-1),\ldots,\hat{\boldsymbol{\phi}}_r(k-m)]$, and $\delta\in(0,1]$ is introduced to avoid the case that the denominator is zero.

Remark 4: For the control variable $\mathbf{U}_r(k)$, it should be noted that $\mathbf{G}_r(k+i)$ and $z_{\bar{r},r}(k+i)$, $i=0,\ldots,M-1$ will be derived by solving an optimization problem, as will be explained in the next step, while $\mathbf{N}_r(k)$ and $\mathbf{N}_{r,\bar{r}}(k)$ can be directly measured by the traffic detectors at time step k without the need of solving an optimization problem. On the other hand, it is noted that $\mathbf{N}_r(k+i)$ and $\mathbf{N}_{r,\bar{r}}(k+i)$ for $i=1,\ldots,M-1$ cannot be obtained by the traffic detectors at each time step k directly. In this case, we can use the same forecasting method as in (22) and (23) to forecast these values.

Remark 5: By virtue of the traffic detectors, the real-time traffic data and past system information can be directly utilized to estimate the pseudogradient $\boldsymbol{\phi}_r(k+i)$, $i=1,\ldots,M$ without using any information of a mathematical traffic model, as seen in (21)–(23). Furthermore, by representing the urban traffic dynamics of $n_r(k)$ shown by (4), (12), and (13) into the MFAPC data model (19), some imprecise problems in existing linearization methods, such as the dropout of high-order terms in Taylor's linearization [43] and the requirement of model information in piecewise linearization [44], can be avoided.

On the other hand, the dynamics of $y_{r,\bar{r}}(k)$ for $r=1,2$, $\bar{r}=3-r$ can also be transformed into a form similar to (17) as follows based on (16):

$$\begin{aligned}y_{r,\bar{r}}(k+1)=&f_y\big(y_{r,\bar{r}}(k),\ldots,y_{r,\bar{r}}(k-\gamma_y),\\&\mathbf{u}_{r,\bar{r}}(k),\ldots,\mathbf{u}_{r,\bar{r}}(k-\gamma_b)\big)\end{aligned} \tag{24}$$

where $\mathbf{u}_{r,\bar{r}}(k)=[(\mathbf{G}_{r,\bar{r}}^{\mathrm{B}}(k))^{\mathrm{T}},\mathbf{N}_{r,\bar{r}}^{\mathrm{T}}(k)]^{\mathrm{T}}$, and γ_y and γ_b are the memory lengths of system (24).

Afterward, the CFDL data model for (24) can be derived. First, the following two assumptions are made on $f_y(\cdot)$.

Assumption 4: The partial derivatives of $f_y(\cdot)$ with respect to every entry of the variable $\mathbf{u}_{r,\bar{r}}(k)$ are continuous.

Assumption 5: The above system satisfies the generalized Lipschitz condition given in the following:

There exists a positive constant $c_{r,\bar{r}}$ such that

$$\left|y_{r,\bar{r}}(k_1+1)-y_{r,\bar{r}}(k_2+1)\right|\le c_{r,\bar{r}}\left\|\mathbf{u}_{r,\bar{r}}(k_1)-\mathbf{u}_{r,\bar{r}}(k_2)\right\|_2$$

for $\mathbf{u}_{r,\bar{r}}(k_1)\neq\mathbf{u}_{r,\bar{r}}(k_2)$ for any $k_1,k_2>0$ with $k_1\neq k_2$.

These two assumptions are similar to Assumptions 2 and 3. Then, the expression (24) can be transformed into the following MISO-CFDL data model:

$$\begin{aligned}y_{r,\bar{r}}(k+1)&=y_{r,\bar{r}}(k)+\boldsymbol{\varphi}_{r,\bar{r}}(k)\Delta\mathbf{u}_{r,\bar{r}}(k)\\ \boldsymbol{\varphi}_{r,\bar{r}}(k)&=\left[\boldsymbol{\varphi}_1(k),\ldots,\boldsymbol{\varphi}_{q_{r,\bar{r}}}(k),\boldsymbol{\varphi}_{q_{r,\bar{r}}+1}(k),\ldots,\boldsymbol{\varphi}_{q_{r,\bar{r}}+h_{r,\bar{r}}}(k)\right]^{\mathrm{T}}\end{aligned} \tag{25}$$

where $q_{r,\bar{r}}$ is the total number of signal phases of intersections in region r at the boundary with region $\bar{r}$ and $h_{r,\bar{r}}$ is the total number of links on which vehicles travel from region r to $\bar{r}$.

In a similar way as (19), (25) can be further rewritten as the following prediction equation:

$$\mathbf{Y}_{r,\bar{r}}(k+1) = \mathbf{E}y_{r,\bar{r}}(k) + \mathbf{A}_{r,\bar{r}}(k)\Delta\mathbf{U}_{r,\bar{r}}(k) \tag{26}$$

where

$$\mathbf{Y}_{r,\bar{r}}(k+1) = \left[y_{r,\bar{r}}(k+1), \ldots, y_{r,\bar{r}}(k+M)\right]^{\mathrm{T}}$$
$$\Delta\mathbf{U}_{r,\bar{r}}(k) = \left[\Delta\mathbf{u}_{r,\bar{r}}^{\mathrm{T}}(k), \ldots, \Delta\mathbf{u}_{r,\bar{r}}^{\mathrm{T}}(k+M-1)\right]^{\mathrm{T}}$$
$$\mathbf{A}_{r,\bar{r}}(k) = \begin{bmatrix} \boldsymbol{\varphi}_{r,\bar{r}}^{\mathrm{T}}(k) & \mathbf{0}^{\mathrm{T}} & \cdots & \mathbf{0}^{\mathrm{T}} \\ \boldsymbol{\varphi}_{r,\bar{r}}^{\mathrm{T}}(k) & \boldsymbol{\varphi}_{r,\bar{r}}^{\mathrm{T}}(k+1) & \cdots & \mathbf{0}^{\mathrm{T}} \\ \vdots & \vdots & \ddots & \vdots \\ \underbrace{\boldsymbol{\varphi}_{r,\bar{r}}^{\mathrm{T}}(k) & \boldsymbol{\varphi}_{r,\bar{r}}^{\mathrm{T}}(k+1) & \cdots & \boldsymbol{\varphi}_{r,\bar{r}}^{\mathrm{T}}(k+M-1)}_{M\times[(q_{r,\bar{r}}+h_{r,\bar{r}})M]} \end{bmatrix}.$$

Similar to (21), $\boldsymbol{\varphi}_{r,\bar{r}}(k)$ in (26) can be determined by

$$\hat{\boldsymbol{\varphi}}_{r,\bar{r}}(k) = \hat{\boldsymbol{\varphi}}_{r,\bar{r}}(k-1) + \frac{\eta_{r,\bar{r}}\Delta\mathbf{u}_{r,\bar{r}}(k-1)}{\mu_{r,\bar{r}} + \left\|\Delta\mathbf{u}_{r,\bar{r}}(k-1)\right\|_2^2} \left(y_{r,\bar{r}}(k) - y_{r,\bar{r}}(k-1) - \hat{\boldsymbol{\varphi}}_{r,\bar{r}}^{\mathrm{T}}(k-1)\Delta\mathbf{u}_{r,\bar{r}}(k-1)\right) \tag{27}$$

where $\mu_{r,\bar{r}} > 0$, $\eta_{r,\bar{r}} \in (0, 1]$. Then, the estimates of $\boldsymbol{\varphi}_{r,\bar{r}}(k+1), \ldots, \boldsymbol{\varphi}_{r,\bar{r}}(k+M-1)$ are given as

$$\begin{aligned}\hat{\boldsymbol{\varphi}}_{r,\bar{r}}(k+i) = {} & \vartheta_1(k)\hat{\boldsymbol{\varphi}}_{r,\bar{r}}(k+i-1) + \vartheta_2(k)\hat{\boldsymbol{\varphi}}_{r,\bar{r}}(k+i-2) \\ & + \cdots + \vartheta_m(k)\hat{\boldsymbol{\varphi}}_{r,\bar{r}}(k+i-m) \\ & i = 1, \ldots, M-1\end{aligned} \tag{28}$$

where $\boldsymbol{\vartheta}(k) = [\vartheta_1(k), \ldots, \vartheta_m(k)]^{\mathrm{T}}$ can be derived by utilizing the same algorithm as in (23).

C. Controller Design of D-MFAPC

The purpose of the D-MFAPC strategy is to reduce the total time spent by vehicles, as well as to improve the traffic efficiency in the network. In this case, the following cost function can be adopted for a two-region urban traffic network:

$$\min J = \sum_{r=1}^{2}\left(\sum_{i=1}^{M} n_r(k+i)\cdot T + \alpha\sum_{i=1}^{M}\max\left(0, n_r(k+i) - n_r^{\mathrm{set}}\right)^2\right) \tag{29}$$

or equivalently

$$\begin{aligned}\min J = {} & \sum_{r=1}^{2}\left(\sum_{i=1}^{M} n_r(k+i)\cdot T + \alpha\sum_{i=1}^{M}\left(\Delta_r(k+i)\right)^2\right) \\ & \text{with } \Delta_r(k+i) \geq n_r(k+i) - n_r^{\mathrm{set}} \\ & \Delta_r(k+i) \geq 0\end{aligned} \tag{30}$$

where $0 < \alpha < 1$. The first term of (29) aims to minimize the total time spent in the network. The second term aims to reduce congestion imposing a penalty of the number of vehicles in a region exceeds the predefined set point n_r^{set}; appropriate values for the set points can be determined off-line based on the macroscopic fundamental diagram (MFD) [45], [46].

Then, the control problem of (30) could be decomposed into two individual optimization problems expressed as follows:

$$\min_{\substack{\mathbf{G}_r(k),\ldots,\mathbf{G}_r(k+M-1)\\ \mathbf{Z}_{\bar{r},r}(k),\mathbf{Y}_{r,\bar{r}}(k)}} J_r = \sum_{i=1}^{M} n_r(k+i)\cdot T + \alpha\sum_{i=1}^{M}\left(\Delta_r(k+i)\right)^2 \tag{31}$$

$$\text{s.t. } \Theta_r(k+1) = \mathbf{E}n_r(k) + \mathbf{A}_r(k)\Delta\mathbf{U}_r(k) \tag{32}$$

$$\mathbf{Y}_{r,\bar{r}}(k+1) = \mathbf{E}y_{r,\bar{r}}(k) + \mathbf{A}_{r,\bar{r}}(k)\Delta\mathbf{U}_{r,\bar{r}}(k) \tag{33}$$

$$(21) - (23), (27) - (28)$$

$$\mathbf{Z}_{\bar{r},r}(k) = \mathbf{Y}_{\bar{r},r}(k) \tag{34}$$

$$\Omega(\mathbf{G}_r(k+i)) = 0 \tag{35}$$

$$\mathbf{G}_{r,\min} \leq \mathbf{G}_r(k+i) \leq \mathbf{G}_{r,\max} \tag{36}$$

$$\Delta_r(k+i) \geq n_r(k+i) - n_r^{\mathrm{set}} \tag{37}$$

$$\Delta_r(k+i) \geq 0 \tag{38}$$

$$\text{for } r = 1, 2, \bar{r} = 3 - r, i = 1, \ldots, M$$

where $\mathbf{Z}_{\bar{r},r}(k) = \left[z_{\bar{r},r}(k), \ldots, z_{\bar{r},r}(k+M-1)\right]^{\mathrm{T}}$. Constraints (32) and (33) are the MFAPC data models of $n_r(k)$ and $y_{r,\bar{r}}(k)$ that have been elaborated in Section III-B. Constraints (21)–(23), (27), and (28) are utilized to determine the pseudo-gradients of the traffic system. Constraint (34) is the interaction constraint, which ensures that the interaction input of region r caused by region $\bar{r}$ equals the interaction output of region $\bar{r}$ on region r. Moreover, $\Omega(\cdot)$ represents the cycle time constraints for all intersections in region r; $\mathbf{G}_{r,\min}$ and $\mathbf{G}_{r,\max}$ are the vectors of minimum and maximum values for all signal phases in region r, respectively. After deriving the optimal control inputs at time step k, only $\mathbf{G}_r(k)$ should be implemented by the traffic lights.

It is easy to verify that optimization problem (31)–(38) is a convex quadratic programming (QP) problem, which can be solved efficiently by QP solvers. Furthermore, one can see from (31)–(38) that all the information used to compute $\Theta_r(k+1)$, $\mathbf{Y}_{r,\bar{r}}(k+1)$, $\mathbf{A}_r(k)$, and $\mathbf{A}_{r,\bar{r}}(k)$ can be directly measured by the traffic detectors without the need of any mathematical traffic model.

However, it should be noted that $\mathbf{Y}_{\bar{r},r}(k)$ in (34) of the control problem of region r is the interaction output variable of another region $\bar{r}$. Thus, the constraint (34) cannot be added directly into the individual optimization problem of region r. Therefore, a negotiation process is needed to satisfy the interaction constraint (34), and this process can be dealt with by the ADMM-based DMPC approach [33]. The detailed procedure of the D-MFAPC strategy at each time step k is summarized in Algorithm 1.

According to Algorithm 1, the two regions solve their own local optimization problems in a distributed and iterative manner at each time step k. At each iteration s, region 1 solves its local problem (39) and sends the derived values of its interaction inputs $z_{2,1}^s(k+i)$ and outputs $y_{1,2}^s(k+i)$ to region 2, and at the same time, it receives $z_{1,2}^s(k+i)$ and $y_{2,1}^s(k+i)$ from region 2. Simultaneously, region 2 performs the same actions for region 1 in a similar manner. Then, the two regions update the values of their associated Lagrangian multipliers $\lambda_{\mathrm{in},\bar{r},r}^s(k)$ and $\lambda_{\mathrm{out},r,\bar{r}}^s(k)$ based on (40) for use at the next iteration.

Algorithm 1 D-MFAPC Strategy for a Two-Region Urban Traffic Network Based on the ADMM-Based DMPC Approach

Input: $n_r(k)$, $\mathbf{N}_r(k)$, $\mathbf{N}_{r,\bar{r}}(k)$ for $r=1,2$, $\bar{r}=3-r$; maximum computation time $T_{\max}$; iteration stopping threshold $\varepsilon_{\text{stop}}$; positive parameter ρ.

Initialization: iteration counter $s \leftarrow 1$, total computation time $t_r(k) \leftarrow 0$ spent by region $r=1,2$ for time step k. The vectors of Lagrangian multipliers $\boldsymbol{\lambda}^s_{\text{in},\bar{r},r}(k) = \left[\lambda^s_{\text{in},\bar{r},r}(k+i)\right]_{i=0,\cdots,M-1}$ and $\boldsymbol{\lambda}^s_{\text{out},r,\bar{r}}(k) = \left[\lambda^s_{\text{out},r,\bar{r}}(k+i)\right]_{i=0,\cdots,M-1}$ for $r=1,2$, $\bar{r}=3-r$ are initialized as zero vectors when $k=1$, and are initialized by using a warm start strategy, i.e., initialized with values obtained from the previous control step [29] when $k>1$. Maximum absolute difference among the values of the Lagrangian multipliers at iteration s and its previous iteration $\varepsilon^s \leftarrow \infty$.

while $\varepsilon^s \geq \varepsilon_{\text{stop}}$ and $\max_{r=1,2} t_r(k) \leq T_{\max}$ **do**

if $s=1$ **then** $\mathbf{D}^s_{\bar{r},r}(k) \leftarrow \mathbf{0}_{M\times 1}$ and $\mathbf{D}^s_{r,\bar{r}}(k) \leftarrow \mathbf{0}_{M\times 1}$

end if

for region $r=1,2$ in a parallel fashion **do**

Compute $\mathbf{G}^{s+1}_r(k+i)$, $z^{s+1}_{\bar{r},r}(k+i)$, $y^{s+1}_{r,\bar{r}}(k+i)$, $i=0,\cdots,M-1$ for the local DMPC problem given by

$$\min_{\substack{\mathbf{G}_r(k),\cdots,\mathbf{G}_r(k+M-1)\\ z_{\bar{r},r}(k),\cdots,z_{\bar{r},r}(k+M-1)\\ y_{r,\bar{r}}(k),\cdots,y_{r,\bar{r}}(k+M-1)}} \left(J_r + \begin{bmatrix} \boldsymbol{\lambda}^s_{\text{in},\bar{r},r}(k) \\ \boldsymbol{\lambda}^s_{\text{out},r,\bar{r}}(k) \end{bmatrix}^{\mathrm{T}} \begin{bmatrix} \mathbf{Z}_{\bar{r},r}(k) \\ \mathbf{Y}_{r,\bar{r}}(k) \end{bmatrix} + \frac{\rho}{2} \left\| \begin{bmatrix} \mathbf{Z}_{\bar{r},r}(k) - \mathbf{D}^s_{\bar{r},r}(k) \\ \mathbf{Y}_{r,\bar{r}}(k) - \mathbf{D}^s_{r,\bar{r}}(k) \end{bmatrix} \right\|_2^2 \right) \tag{39}$$

subject to the dynamics (21)-(23), (27)-(28), (32)-(33), (35)-(38)

Send $\mathbf{Z}^{s+1}_{\bar{r},r}(k)$ and $\mathbf{Y}^{s+1}_{r,\bar{r}}(k)$ to region $\bar{r}=3-r$ and in parallel receive $\mathbf{Z}^{s+1}_{r,\bar{r}}(k)$ and $\mathbf{Y}^{s+1}_{\bar{r},r}(k)$ from region $\bar{r}$

Compute $\mathbf{D}^{s+1}_r(k) = \begin{bmatrix} \mathbf{D}^{s+1}_{\bar{r},r}(k) \\ \mathbf{D}^{s+1}_{r,\bar{r}}(k) \end{bmatrix} \leftarrow \frac{1}{2}\left(\begin{bmatrix} \mathbf{Z}^{s+1}_{\bar{r},r}(k) \\ \mathbf{Y}^{s+1}_{r,\bar{r}}(k) \end{bmatrix} + \begin{bmatrix} \mathbf{Y}^{s+1}_{\bar{r},r}(k) \\ \mathbf{Z}^{s+1}_{r,\bar{r}}(k) \end{bmatrix} \right)$

end for

Update $\boldsymbol{\lambda}^s_{\text{in},\bar{r},r}(k)$ and $\boldsymbol{\lambda}^s_{out,r,\bar{r}}(k)$ for $r=1,2$, $\bar{r}=3-r$

$$\begin{bmatrix} \boldsymbol{\lambda}^{s+1}_{\text{in},\bar{r},r}(k) \\ \boldsymbol{\lambda}^{s+1}_{\text{out},r,\bar{r}}(k) \end{bmatrix} \leftarrow \begin{bmatrix} \boldsymbol{\lambda}^s_{\text{in},\bar{r},r}(k) \\ \boldsymbol{\lambda}^s_{\text{out},r,\bar{r}}(k) \end{bmatrix} + \rho \left(\begin{bmatrix} \mathbf{Z}^{s+1}_{\bar{r},r}(k) \\ \mathbf{Y}^{s+1}_{r,\bar{r}}(k) \end{bmatrix} - \begin{bmatrix} \mathbf{D}^{s+1}_{\bar{r},r}(k) \\ \mathbf{D}^{s+1}_{r,\bar{r}}(k) \end{bmatrix} \right) \tag{40}$$

Update total computation time $t_r(k)$ for $r=1,2$

Compute $\varepsilon^{s+1} \leftarrow \max_{r=1,2} \left\| \begin{bmatrix} \boldsymbol{\lambda}^{s+1}_{\text{in},\bar{r},r}(k) - \boldsymbol{\lambda}^s_{\text{in},\bar{r},r}(k) \\ \boldsymbol{\lambda}^{s+1}_{\text{out},r,\bar{r}}(k) - \boldsymbol{\lambda}^s_{\text{out},r,\bar{r}}(k) \end{bmatrix} \right\|_\infty$

$s \leftarrow s+1$

end while

Output: $\mathbf{G}_r(k+i)$, $z_{\bar{r},r}(k+i)$, $y_{r,\bar{r}}(k+i)$ for $r=1,2$, $\bar{r}=3-r$, $i=0,\cdots,M-1$

The two regions repeat the same procedure iteratively until the stopping criterion is triggered.

IV. Case Study

A. Traffic Network and Evaluation Criteria for the Case Study

To assess the proposed D-MFAPC strategy, the traffic network from Linfen, Shanxi, China, is considered. The network is represented in Fig. 2, and it is composed of 23 intersections, 102 links, and 16 vehicle inflow points $V_1 - V_{16}$. In Fig. 2, the length of each link has been indicated besides the link (in meters). Each crossroad has four signal phases, and each T-intersection has three signal phases, with in total 86 signal phases in the whole network. The network is simulated using VISSIM [47] with control algorithms programmed in MATLAB.

The sampling interval, control interval, and common cycle length of all intersections are set as $T = 120$ s, and the total simulation time period is 12 000 s, which corresponds to 100 control intervals. The simulation period corresponds to the evening rush hour of Linfen, Shanxi, China. The detailed traffic demand of the network provided by the Linfen Traffic Management Bureau is listed in Table II. The origin–destination matrix and paths of the vehicles are predefined and fixed in the case study based on the traffic data provided by the traffic management bureau, regardless of the real-time traffic condition of the network and the control strategy being used.

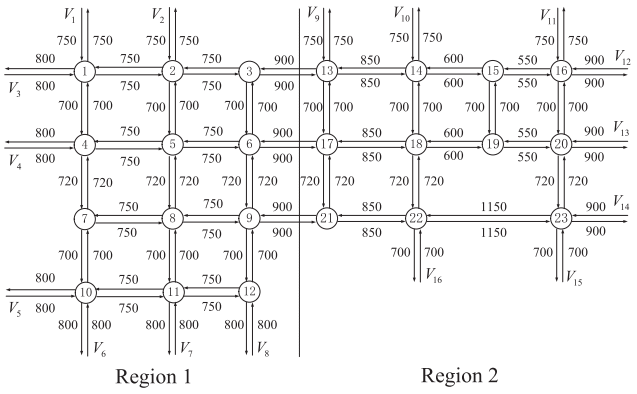

Fig. 2. Traffic network of Linfen, Shanxi, China.

TABLE II
TRAFFIC DEMAND OF THE NETWORK (IN VEH/H)

vehicle input points	Period of time (s)		
	0-2400	2400-7200	7200-12000
1	600	1000	400
2	840	1400	560
3	900	1500	600
4	900	1500	600
5	840	1400	560
6	840	1400	560
7	480	800	320
8	480	800	320
9	540	900	360
10	432	720	288
11	450	750	300
12	510	850	340
13	540	900	360
14	900	1500	600
15	900	1500	600
16	540	900	360

In order to compare the control performance under different strategies, the following evaluation criteria are considered.

1) The total traffic throughput $\mathrm{TTT}(k)$ is the total number of vehicles completing the trip and leaving the network from the start of the simulation to time step k, which can be expressed as

$$\mathrm{TTT}(k) = \sum_{m=1}^{k} n_{\mathrm{leave}}(m) \tag{41}$$

where $n_{\mathrm{leave}}(m)$ is the number of vehicles leaving the network during time interval $[mT, (m+1)T]$.

2) The total time spent $\mathrm{TTS}(k)$ is the cumulative time that all vehicles spent in the traffic network from the start of the simulation to time step k, which is described as

$$\mathrm{TTS}(k) = \sum_{m=1}^{k} T \cdot n(m). \tag{42}$$

3) The average flow rate $\mathrm{AFR}_r(k)$ is defined as the average flow in region r during time interval $[kT, (k+1)T]$, which is expressed as

$$\mathrm{AFR}_r(k) = \frac{\sum_{i \in I_r} \sum_{j \in I_{\mathrm{N},i}} e_{(j,i)}(k)}{T \cdot L_r} \tag{43}$$

where L_r is the total number of links in region r.

4) The total number of vehicles $\mathrm{TNV}_r(k)$ in region r at time step k, which has been defined in (4).

B. Control Strategies and Solver Settings

The performance of the following four control strategies is compared in the case study.

1) *Fixed-Time (FT) Control:* The actual FT signal settings in the peak hours of Linfen city are applied, which is tuned based on off-line traffic data using the well-known Webster method [48].
2) *A Centralized MPC Controller (C-MPC) to Control the Whole Network:* In this strategy, the traffic network is controlled by a single centralized MPC controller that optimizes the signal settings of the entire network dynamically at each time step k. The S model (6)–(9) is utilized as the prediction model of the MPC controller.
3) *A Model-Based DMPC (M-DMPC) Strategy:* The whole urban traffic network is decomposed into two regions 1 and 2 (see Fig. 2). Each region is assigned an MPC controller that solves an independent optimization problem using the S model. Information exchange and negotiations among the regions are solved by the ADMM-based DMPC approach [33].
4) *A Centralized MFAPC (C-MFAPC) Strategy:* In this strategy, the dynamics of shown by (3), (14), and (15) can be represented by an MFAPC data model similar to (19) and (21)–(23). Compared with the C-MPC strategy, the derived MFAPC data model instead of S model is utilized as the prediction model.
5) *The D-MFAPC Strategy Proposed in This Article:* Compared with the M-DMPC strategy, MFAPC data models representing traffic dynamics of the regions instead of a mathematical model are utilized as the prediction models. Specifically, Algorithm 1 is performed at each time step k.

Under all control strategies, the initial traffic condition (i.e., vehicle distribution and signal settings) of the network is the same to ensure the fairness of the simulation. Then, for all nonlinear control approaches (i.e., C-MPC and M-DMPC), we perform a multistart optimization with five different random starting points[1] at each time step k, and we select the best result and use it as control input for time step k.

Based on trial-and-error experiments carried out for this particular problem settings, the prediction and control horizons are set as $M = 8$, and the weighting factor in (31) is set as $\alpha = 0.5$. For the parameters of the ADMM-based DMPC approach shown in Algorithm 1, we have selected $T_{\max} = 30\,\mathrm{min}$, $\rho = 0.8$, and $\varepsilon_{\mathrm{stop}} = 5 \times 10^{-2}$. For the parameters of the MFAPC data models, we have selected $\eta_r = 0.31$, $\eta_{r,\bar{r}} = 0.15$, $\mu_r = 0.008$, $\mu_{r,\bar{r}} = 0.005$, and $\delta = 0.1$ for $r = 1, 2$ which are used in (20), (21), (23), and (27).

To obtain the values of n_1^{set} and n_2^{set} off-line, the MFDs of the regions are needed. In this case study, we use a fifth-order polynomial function to obtain the unimodal MFDs of the regions

$$\begin{aligned}\mathrm{AFR}_r(k) = {} & a_{r,1} n_r^5(k) + a_{r,2} n_r^4(k) + a_{r,3} n_r^3(k) \\ & + a_{r,4} n_r^2(k) + a_{r,5} n_r(k) + a_{r,6}\end{aligned} \tag{44}$$

where $a_{r,1}, \ldots, a_{r,6}$, $r = 1, 2$ are the parameters to be estimated.

The MFDs of the two regions are shown in Fig. 3, which are obtained under FT control tuned using Webster's method. Based on the "polyfit" function in MATLAB, we get the parameters as follows: $a_{1,1} = 2.044 \times 10^{-19}$, $a_{1,2} = -5.811 \times 10^{-15}$, $a_{1,3} = 5.953 \times 10^{-11}$, $a_{1,4} = -2.756 \times 10^{-7}$, $a_{1,5} = 5.578 \times 10^{-4}$, $a_{1,6} = 0.044$ $a_{2,1} = 2.210 \times 10^{-19}$, $a_{2,2} = -6.079 \times 10^{-15}$, $a_{2,3} = 6.255 \times 10^{-11}$, $a_{2,4} = -3.032 \times 10^{-11}$,

[1] In our experiments, this number gave a balanced tradeoff between the computation time and the possibility of ending up in a local minimum.

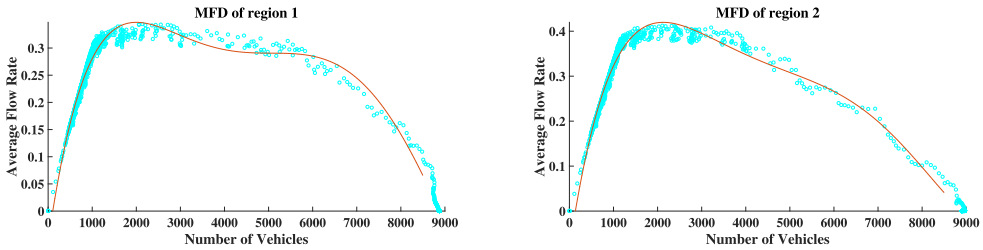

(a) (b)

Fig. 3. MFDs of the regions. (a) Region 1. (b) Region 2.

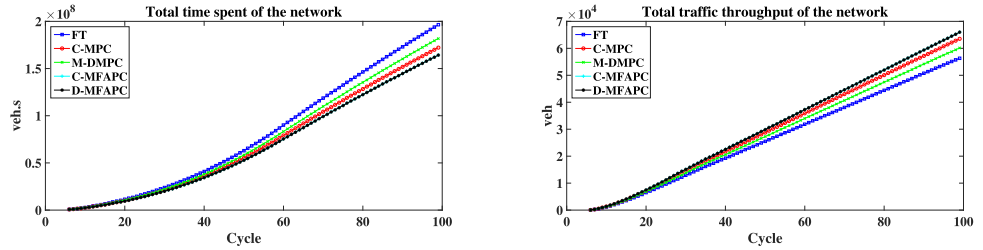

(a) (b)

Fig. 4. Comparison of (a) TTS and (b) TTT of the entire network under different control strategies.

TABLE III
TTT(100) AND TTS(100) OF THE ENTIRE TRAFFIC NETWORK UNDER DIFFERENT CONTROL STRATEGIES

Control strategy	Performance criteria			
	TTT(100) (veh)	Compared with FT	$\mathrm{TTS}_{\mathrm{EN}}(100)$ (s)	Compared with FT
FT	56965	-	1.9886×10^8	-
C-MPC	64209	+12.72%	1.7443×10^8	-12.29%
M-DMPC	61734	+8.37%	1.8233×10^8	-8.31%
C-MFAPC	66678	+17.05%	1.6629×10^8	-16.38%
D-MFAPC	66678	+17.05%	1.6629×10^8	-16.38%

$a_{2,5} = 6.521 \times 10^{-11}$, $a_{2,6} = -0.083$, $n_1^{\mathrm{set}} = 2000$ veh, and $n_2^{\mathrm{set}} = 2127$ veh.

C. Performance Evaluations of the Control Strategies

In this section, the control performance of the different control strategies is compared. More specifically, the simulation results of TTS(k) and TTT(k) of the entire traffic network under different strategies are shown in Fig. 4 and Table III, and the evolution of $\mathrm{AFR}_r(k)$ and $\mathrm{TNV}_r(k)$ of the two regions under different strategies is shown in Fig. 5.

From Fig. 4 and Table III, we can see that the C-MPC strategy has a better performance than M-DMPC because the global optimum can be obtained more easily by utilizing a centralized control structure. Compared with C-MPC, the C-MFAPC strategy can further improve the control performance by directly utilizing the real-time measured traffic data instead of mathematical traffic models, which can avoid the problem of model mismatch and traffic uncertainties in the optimization process. Finally, it can be seen from Fig. 4 and Table III that D-MFAPC and C-MFAPC have exactly the same control performance. This is because the optimal solution of a centralized control problem can be found iteratively by the distributed control scheme with negotiations among the subsystems, under the convexity assumptions on the objective functions and constraints of the problem [29], [49].

Meanwhile, in Fig. 5, it can be seen that during the 40th–80th cycles, i.e., the most congested period, the average flow rates of both regions under the C-MFAPC and the D-MFAPC strategies are larger than under the other three strategies. Furthermore, the number of vehicles in the two regions under the C-MFAPC and the D-MFAPC strategies can better track the set points of n_1^{set} and n_2^{set} compared with the other three strategies, because of the data-driven control characteristics of C-MFAPC and D-MFAPC. We can see from Figs. 4 and 5 and Table III that the simulation results of the individual regions are consistent with the simulation results of the entire network.

D. Illustration of Interaction Process

Now, we present the evolution of the differences between the interaction inputs and the outputs and the evolution of the associated Lagrangian multipliers (introduced in Algorithm 1) of the two regions under the D-MFAPC strategy. In this case study, we take the time step $k = 6$ as an illustrative example. Fig. 6 shows the evolution of the differences of the two sets of interaction variables $z_{2,1}(k+i)$ and $y_{2,1}(k+i)$, $z_{1,2}(k+i)$ and $y_{1,2}(k+i)$ for $i = 0, \ldots, M-1$ for time step $k = 6$, whereas Fig. 7 shows the variation of the Lagrangian multipliers $\lambda_{\mathrm{in},2,1}(k+i)$, $\lambda_{\mathrm{out},1,2}(k+i)$, $\lambda_{\mathrm{in},1,2}(k+i)$, and $\lambda_{\mathrm{out},2,1}(k+i)$ for $i = 0, \ldots, M-1$ for time step $k = 6$.

It can be seen from Fig. 6 that the differences between the interaction variables of the regions are very large in the

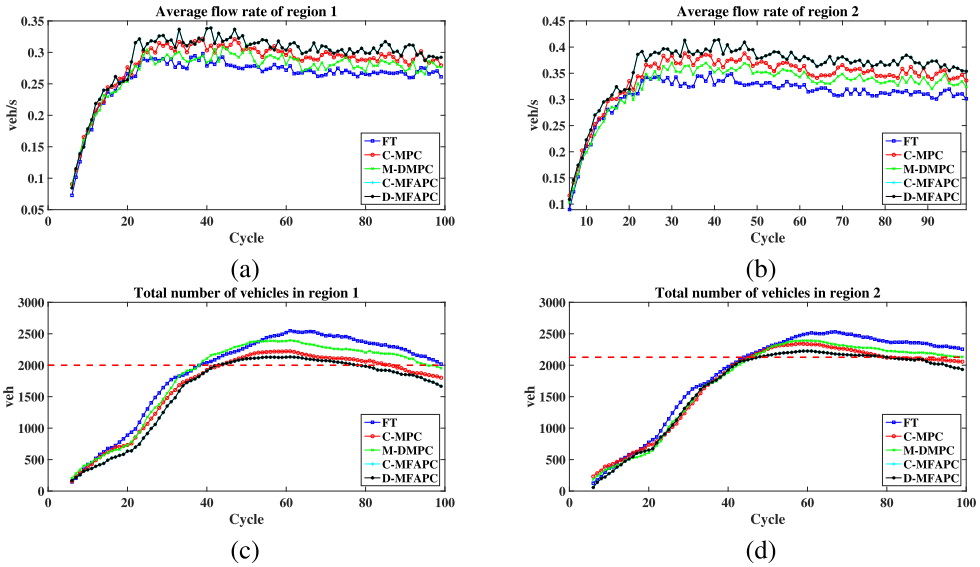

Fig. 5. Comparison of AFR and TNV of the two regions under different control strategies. (a) AFR of region 1. (b) AFR of region 2. (c) TNV of region 1. (d) TNV of region 2.

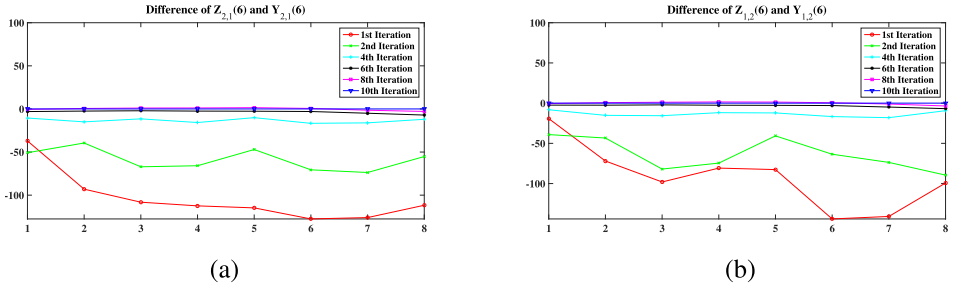

Fig. 6. Evolution of (a) difference of $z_{2,1}(k+i)$ and $y_{2,1}(k+i)$ and (b) difference of $z_{1,2}(k+i)$ and $y_{1,2}(k+i)$ for $i = 0, \ldots, M-1$ for time step $k = 6$ over the prediction period with $M = 8$.

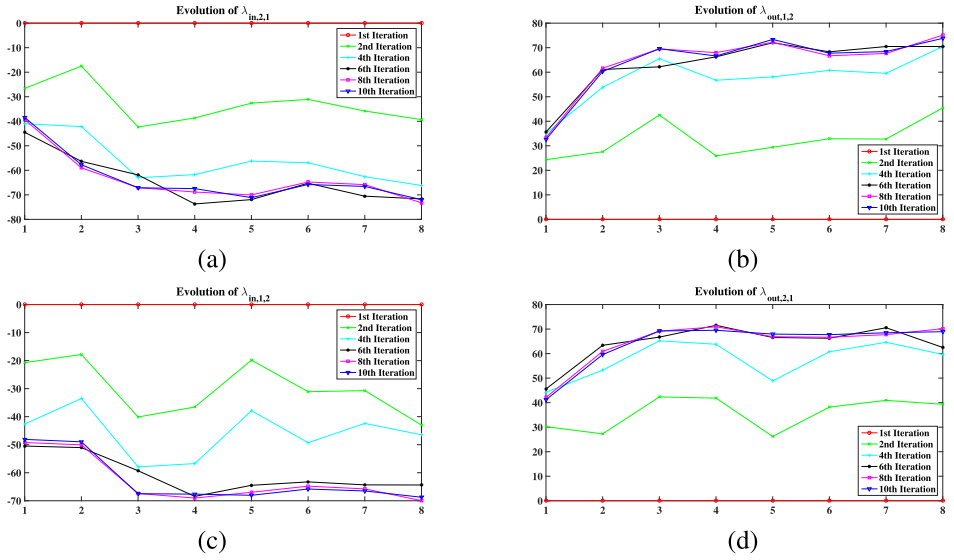

Fig. 7. Evolution of (a) $\lambda_{\text{in},2,1}(k+i)$, (b) $\lambda_{\text{out},1,2}(k+i)$, (c) $\lambda_{\text{in},1,2}(k+i)$, and (d) $\lambda_{\text{out},2,1}(k+i)$ for $i = 0, \ldots, M-1$ for time step $k = 6$ over the prediction period with $M = 8$.

first iteration, but the differences gradually decrease with the increase of the iteration index. At the same time, the values of the Lagrangian multipliers of the two regions are updated according to the differences between the interaction variables, as shown in Fig. 7. The negotiation process between the two regions terminates when the absolute differences between the

TABLE IV
COMPUTATION TIME UNDER DIFFERENT CONTROL STRATEGIES

Control strategy	Total computation time (s)	Average computation time per cycle (s)
FT	-	-
C-MPC	2441	24.41
M-DMPC	1235	12.35
C-MFAPC	598	5.98
D-MFAPC	311	3.11

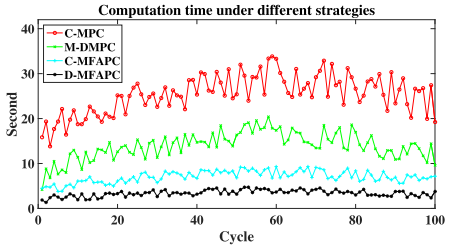

Fig. 8. Evolution of the computation time for the consecutive time steps under different control strategies.

values of their associated Lagrangian multipliers at successive iterations are smaller than the threshold value $\varepsilon_{\text{stop}}$.

E. Comparison of Computation Time

The computation times under different control strategies within the simulation period are presented in Table IV and Fig. 8. These computation times take a distributed implementation into account for M-DMPC and D-MFAPC and are obtained using the "etime" function of MATLAB. The optimization problems are solved in the MATLAB R2016 environment using the "fmincon" function with the "sqp" algorithm for C-MPC and M-DMPC, and the "linprog" function for D-MFAPC on a computer with a 3.50-GHz Intel Xeon CPU E5-1620 v3 and 32-GB RAM.

From Table IV and Fig. 8, we can see that the C-MPC strategy has the largest computation time because a centralized optimization problem with many constraints, involving 86 links, 23 intersections, and 86 signal phases in the entire network, needs to be solved in each time step. On the other hand, M-DMPC can reduce the computation time by half compared with C-MPC by decomposing the whole optimization problem into two smaller and independent problems. The C-MFAPC and the D-MFAPC strategies can further significantly decrease the computation time compared with M-DMPC by utilizing linear MFAPC data models in the control process instead of nonlinear mathematical traffic models. Finally, due to the distributed control characteristics, D-MFAPC requires less computation time compared with the C-MFAPC method.

V. CONCLUSION AND FUTURE WORK

In this article, a novel D-MFAPC strategy for multiregion urban traffic networks is proposed. First, the dynamics of the two-region traffic networks are analyzed, and the MFAPC data models of the regions are derived. Then, the D-MFAPC algorithm is designed using the derived MFAPC data models instead of mathematical traffic models in the control process, which can avoid the problem of model mismatch and dramatically decrease the computational burden.

Simulation results of the traffic network of Linfen, Shanxi, China, show that the proposed D-MFAPC strategy yields a better performance than the FT, the C-MPC, and the M-DMPC strategies. Moreover, the proposed D-MFAPC strategy needs much less computation time than the C-MPC, the M-DMPC, and the centralized MFAPC strategies.

There are still some open problems that can be further explored. First, a more general MFAPC data model suitable for the unsaturated traffic network needs to be established. In addition, more comprehensive objective functions representing the interests of the individual links, the regions, and the whole network, should be designed. Finally, it is worthy to theoretically investigate the stability of the proposed control strategy, e.g., by Lyapunov function-based methods.

REFERENCES

[1] J. Little, M. D. Kelson, and N. H. Gartner, "MAXBAND: A program for setting signals on arteries and triangular networks," *Transp. Res. Rec.*, vol. 795, pp. 40–46, Jun. 1981.
[2] D. Hale, *Traffic Netw. Study Tool—TRANSYT-7F*, McTrans Center of Univ. Florida, Belle Glade, FL, USA, 2005.
[3] C. Diakaki, M. Papageorgiou, and K. Aboudolas, "A multivariable regulator approach to traffic-responsive network-wide signal control," *Control Eng. Pract.*, vol. 10, no. 2, pp. 183–195, Feb. 2002.
[4] C. Diakaki *et al.*, "Extensions and new applications of the traffic-responsive urban control strategy: Coordinated signal control for urban networks," *Transp. Res. Rec., J. Transp. Res. Board*, vol. 1856, no. 1, pp. 202–211, Jan. 2003.
[5] A. Kouvelas, K. Aboudolas, M. Papageorgiou, and E. B. Kosmatopoulos, "A hybrid strategy for real-time traffic signal control of urban road networks," *IEEE Trans. Intell. Transp. Syst.*, vol. 12, no. 3, pp. 884–894, Sep. 2011.
[6] S. Lin, B. De Schutter, Y. Xi, and H. Hellendoorn, "Fast model predictive control for urban road networks via MILP," *IEEE Trans. Intell. Transp. Syst.*, vol. 12, no. 3, pp. 846–856, Sep. 2011.
[7] S. Lin, B. De Schutter, Y. Xi, and H. Hellendoorn, "Efficient network-wide model-based predictive control for urban traffic networks," *Transp. Res. C, Emerg. Technol.*, vol. 24, pp. 122–140, Oct. 2012.
[8] K. Aboudolas, M. Papageorgiou, A. Kouvelas, and E. Kosmatopoulos, "A rolling-horizon quadratic-programming approach to the signal control problem in large-scale congested urban road networks," *Transp. Res. C, Emerg. Technol.*, vol. 18, no. 5, pp. 680–694, Oct. 2010.
[9] K. Aboudolas, M. Papageorgiou, and E. Kosmatopoulos, "Store-and-forward based methods for the signal control problem in large-scale congested urban road networks," *Transp. Res. C, Emerg. Technol.*, vol. 17, no. 2, pp. 163–174, Apr. 2009.
[10] T. Tettamanti, T. Luspay, B. Kulcsar, T. Peni, and I. Varga, "Robust control for urban road traffic networks," *IEEE Trans. Intell. Transp. Syst.*, vol. 15, no. 1, pp. 385–398, Feb. 2014.
[11] Y. Yin, "Robust optimal traffic signal timing," *Transp. Res. B, Methodol.*, vol. 42, no. 10, pp. 911–924, Dec. 2008.
[12] P. Mirchandani and L. Head, "A real-time traffic signal control system: Architecture, algorithms, and analysis," *Transp. Res. C, Emerg. Technol.*, vol. 9, no. 6, pp. 415–432, Dec. 2001.
[13] L. B. de Oliveira and E. Camponogara, "Multi-agent model predictive control of signaling split in urban traffic networks," *Transp. Res. C, Emerg. Technol.*, vol. 18, no. 1, pp. 120–139, Feb. 2010.
[14] Z. Zhou, B. De Schutter, S. Lin, and Y. G. Xi, "Multi-agent model-based predictive control for large-scale urban traffic networks using a serial scheme," *IET Control Theory Appl.*, vol. 9, no. 3, pp. 475–484, 2014.
[15] B.-L. Ye, W. Wu, L. Li, and W. Mao, "A hierarchical model predictive control approach for signal splits optimization in large-scale urban road networks," *IEEE Trans. Intell. Transp. Syst.*, vol. 17, no. 8, pp. 2182–2192, Aug. 2016.

[16] Z. Zhou, B. De Schutter, S. Lin, and Y. Xi, "Two-level hierarchical model-based predictive control for large-scale urban traffic networks," *IEEE Trans. Control Syst. Technol.*, vol. 25, no. 2, pp. 496–508, Mar. 2017.
[17] Z. S. Hou, "The parameter identification, adaptive control and model free learning adaptive control for nonlinear systems," Ph.D. dissertation, Northeastern Univ., Shenyang, China, 1994.
[18] Z. S. Hou and S. T. Jin, *Model Free Adaptive Control: Theory and Applications*. Boca Raton, FL, USA: CRC Press, 2013.
[19] Y. Ma, X. Wang, Z. Quan, and H. V. Poor, "Data-driven measurement of receiver sensitivity in wireless communication systems," *IEEE Trans. Commun.*, vol. 67, no. 5, pp. 3665–3676, May 2019.
[20] M. Fetanat, M. Stevens, C. Hayward, and N. H. Lovell, "A physiological control system for an implantable heart pump that accommodates for interpatient and intrapatient variations," *IEEE Trans. Biomed. Eng.*, vol. 67, no. 4, pp. 1167–1175, Apr. 2020.
[21] Y. Zhu, Z. Hou, F. Qian, and W. Du, "Dual RBFNNs-based model-free adaptive control with aspen HYSYS simulation," *IEEE Trans. Neural Netw. Learn. Syst.*, vol. 28, no. 3, pp. 759–765, Mar. 2017.
[22] D. Li and Z. Hou, "Perimeter control of urban traffic networks based on model-free adaptive control," *IEEE Trans. Intell. Transp. Syst.*, early access, Jun. 4, 2020, doi: 10.1109/TITS.2020.2992337.
[23] T. Lei, Z. Hou, and Y. Ren, "Data-driven model free adaptive perimeter control for multi-region urban traffic networks with route choice," *IEEE Trans. Intell. Transp. Syst.*, vol. 21, no. 7, pp. 2894–2905, Jul. 2020, doi: 10.1109/TITS.2019.2921381.
[24] Y. Ren, Z. Hou, I. I. Sirmatel, and N. Geroliminis, "Data driven model free adaptive iterative learning perimeter control for large-scale urban road networks," *Transp. Res. C, Emerg. Technol.*, vol. 115, Jun. 2020, Art. no. 102618, doi: 10.1016/j.trc.2020.102618.
[25] Z. Hou, R. Chi, and H. Gao, "An overview of dynamic-linearization-based data-driven control and applications," *IEEE Trans. Ind. Electron.*, vol. 64, no. 5, pp. 4076–4090, May 2017.
[26] Z. Hou and S. Xiong, "On model-free adaptive control and its stability analysis," *IEEE Trans. Autom. Control*, vol. 64, no. 11, pp. 4555–4569, Nov. 2019.
[27] J. M. Maestre and R. R. Negenborn, *Distributed Model Predictive Control Made Easy*. Berlin, Germany: Springer, 2014.
[28] P. D. Christofides, R. Scattolini, D. Muñoz de la Peña, and J. Liu, "Distributed model predictive control: A tutorial review and future research directions," *Comput. Chem. Eng.*, vol. 51, pp. 21–41, Apr. 2013.
[29] R. R. Negenborn, B. De Schutter, and J. Hellendoorn, "Multi-agent model predictive control for transportation networks: Serial versus parallel schemes," *Eng. Appl. Artif. Intell.*, vol. 21, no. 3, pp. 353–366, Apr. 2008.
[30] S. Boyd, "Distributed optimization and statistical learning via the alternating direction method of multipliers," *Found. Trends Mach. Learn.*, vol. 3, no. 1, pp. 1–122, 2010.
[31] P. Mc Namara, R. R. Negenborn, B. De Schutter, and G. Lightbody, "Optimal coordination of a multiple HVDC link system using centralized and distributed control," *IEEE Trans. Control Syst. Technol.*, vol. 21, no. 2, pp. 302–314, Mar. 2013.
[32] V. Spudić, C. Conte, M. Baotić, and M. Morari, "Cooperative distributed model predictive control for wind farms," *Optim. Control Appl. Methods*, vol. 36, no. 3, pp. 333–352, May 2015.
[33] L. Li, R. R. Negenborn, and B. De Schutter, "Distributed model predictive control for cooperative synchromodal freight transport," *Transp. Res. E: Logistics Transp. Rev.*, vol. 105, pp. 240–260, Sep. 2017.
[34] Y. Ji and N. Geroliminis, "On the spatial partitioning of urban transportation networks," *Transp. Res. B, Methodol.*, vol. 46, no. 10, pp. 1639–1656, Dec. 2012.
[35] M. Saeedmanesh and N. Geroliminis, "Clustering of heterogeneous networks with directional flows based on 'Snake' similarities," *Transp. Res. B, Methodol.*, vol. 91, pp. 250–269, Sep. 2016.
[36] Z. Zhou, S. Lin, and Y. Xi, "A dynamic network partition method for heterogenous urban traffic networks," in *Proc. 15th Int. IEEE Conf. Intell. Transp. Syst.*, Anchorage, AK, USA, Sep. 2012, pp. 820–825.
[37] A. Jamshidnejad, S. Lin, Y. Xi, and B. De Schutter, "Corrections to 'integrated urban traffic control for the reduction of travel delays and emissions' [Dec 13 1609-1619]," *IEEE Trans. Intell. Transp. Syst.*, vol. 20, no. 5, pp. 1978–1983, May 2019.
[38] D. Gazis and R. Potts, "The oversaturated intersection," in *Proc. 2nd. Int. Symp. Traffic Theory*, London, U.K., 1963, pp. 221–237.
[39] M. van den Berg, A. Hegyi, B. D. Schutter, and J. Hellendoorn, "Integrated traffic control for mixed urban and freeway networks: A model predictive control approach," *Eur. J. Transp. Infrastruct. Res.*, vol. 7, no. 3, pp. 223–250, Sep. 2007.
[40] S. Lin and Y. Xi, "An efficient model for urban traffic network control," *IFAC Proc. Volumes*, vol. 41, no. 2, pp. 14066–14071, 2008.
[41] A. Jamshidnejad, I. Papamichail, M. Papageorgiou, and B. De Schutter, "Sustainable model-predictive control in urban traffic networks: Efficient solution based on general smoothening methods," *IEEE Trans. Control Syst. Technol.*, vol. 26, no. 3, pp. 813–827, May 2018.
[42] Z. Han, "On the identification of time-varying parameters in dynamic systems," *Acta Autom. Sinica*, vol. 10, no. 4, pp. 330–337, 1984.
[43] L. Chen and K. S. Narendra, "Identification and control of a nonlinear discrete-time system based on its linearization: A unified framework," *IEEE Trans. Neural Netw.*, vol. 15, no. 3, pp. 663–673, May 2004.
[44] Y. G. Xi, F. Wang, and G. H. Wu, "Nonlinear multi-model predictive control," *IFAC Proc. Volumes*, vol. 29, no. 1, pp. 2359–2364, 1996.
[45] J. W. Godfrey, "The mechanism of a road network," *Traffic Eng. Control*, vol. 11, no. 7, pp. 323–327, 1969.
[46] N. Geroliminis and C. F. Daganzo, "Existence of urban-scale macroscopic fundamental diagrams: Some experimental findings," *Transp. Res. B, Methodol.*, vol. 42, no. 9, pp. 759–770, Nov. 2008.
[47] *VISSIM 9-User Manual*, PTV, Karlsruhe, Germany, 2016.
[48] F. V. Webster, "Traffic signal settings," Road Res. Lab., Crowthorne, U.K., Tech. Paper 39, 1958.
[49] D. P. Bertsekas, *Constrained Optimization and Lagrange Multiplier Methods*. London, U.K.: Academic, 1982.

Dai Li received the bachelor's degree from Beijing Jiaotong University, Beijing, China, in 2011, and the master's degree from the North China University of Technology, Beijing, in 2014. He is currently pursuing the Ph.D. degree in control science and control engineering with the Advanced Control Systems Laboratory, School of Electronic and Information Engineering, Beijing Jiaotong University.

His research interests include data-driven control, and modeling and control of urban traffic network.

Bart De Schutter (Fellow, IEEE) received the Ph.D. degree in applied sciences from KU Leuven, Leuven, Belgium, in 1996.

He is currently a Full Professor and the Head of the Department at the Delft Center for Systems and Control, Delft University of Technology, Delft, The Netherlands. His current research interests include multilevel and distributed control, and intelligent transportation systems.

Dr. De Schutter is a Senior Editor of the IEEE TRANSACTIONS ON INTELLIGENT TRANSPORTATION SYSTEMS and an Associate Editor of IEEE TRANSACTIONS ON AUTOMATIC CONTROL.